

Photoelectron Spectroscopy of SO_3^- at 355 and 266 nm

S. Dobrin, B. H. Boo,[†] L. S. Alconcel, and R. E. Continetti*

Department of Chemistry and Biochemistry, University of California, San Diego, 9500 Gilman Drive, La Jolla, California 92093-0314

Received: July 19, 2000; In Final Form: September 11, 2000

Photoelectron spectra of SO_3^- were recorded at 266 and 355 nm to study photodetachment of the SO_3^- anion (${}^2\text{A}_1$) to the ground state of neutral SO_3 (${}^1\text{A}'_1$). A long vibrational progression in the 355 nm spectrum is attributed to excitation of the umbrella mode, ν_2 , consistent with predictions that C_{3v} symmetry SO_3^- yields D_{3h} symmetry SO_3 upon photodetachment. At 266 nm, photodissociation of SO_3^- to $\text{SO}_2 + \text{O}^-$ was also observed. The geometry and normal-mode frequencies of SO_3^- and SO_3 as well as the adiabatic electron affinity (AEA) and vertical detachment energy (VDE) of SO_3 have also been calculated with ab initio (MP2 and CCSD(T)) and DFT methods. Using theoretical predictions and experimental data, Franck–Condon simulations of the photoelectron spectra were found to be in good agreement with experiment. The calculated AEA agreed well with experiment, but the VDE was found to be less accurate, presumably because of the large geometry change between anion and neutral.

1. Introduction

The structure and energetics of the sulfur oxides are of interest due to the important role played by these species in a variety of environmental problems. Among them, sulfur trioxide (SO_3) has attracted attention as an intermediate in the conversion of SO_2 to H_2SO_4 , forming acid rain.¹ The kinetics and mechanism of this reaction have been intensively studied experimentally^{2–4} and theoretically.^{5–8} Despite the reactivity of SO_3 , a number of studies have shown that it is a planar molecule with D_{3h} symmetry in the ground state. These studies have included infrared, Raman and photoionization studies of gas-phase SO_3 ^{9–13} and laser flash photolysis and infrared studies in matrix isolation experiments.^{14,15} In the matrix isolation experiments, several isomers of SO_3 have also been identified.¹⁵ These experimental studies have been complemented by a number of ab initio calculations on the ground electronic state of SO_3 .^{7,8} The most recent of these include a detailed study of the thermochemistry and calculation of a spectroscopic quality force field for SO_3 using the CCSD(T) method and large basis sets including inner-shell correlation by Martin.^{16,17}

The SO_3^- anion, however, has received considerably less attention. Experimentally, the UV absorption spectrum of the anion was measured by pulsed radiolysis¹⁸ and matrix-isolation FTIR studies have been carried out.¹⁹ The electron affinity of SO_3 has been measured by collisional ionization²⁰ and in electron-transfer experiments between SO_3^- and various collision partners.²¹ An unresolved portion of the SO_3^- photoelectron spectrum at 355 nm was recently reported by Ding, et al. in a study of the doubly charged $\text{S}_2\text{O}_8^{2-}$ anions.²² Theoretical studies of the SO_3^- anion to date have been carried out at relatively low levels using small basis sets and approximate methods. Margrave and co-workers carried out UHF SCF/3-21+G* calculations to aid in the interpretation of matrix-isolation FTIR spectra.¹⁹ More recently, in a study of mono- and di-sulfoxy

anions, McKee performed DFT/6-31+G(d) and post-Hartree–Fock (MP2, G2, QCISD(T)) calculations with the same basis set, yielding values for the adiabatic electron affinity of SO_3 ranging from 2.15 to 2.50 eV.²³ These calculations also show the anion to be pyramidal with C_{3v} symmetry.

In the present study, photoelectron spectra of SO_3^- have been measured at 355 and 266 nm. It is found in the photoelectron spectra that photodetachment of pyramidal SO_3^- produces SO_3 far from the equilibrium geometry, leading to significant excitation of the out-of-plane bending motion (i.e., ν_2 or “umbrella” mode). As demonstrated by Ellison et al. in a study of CH_3 and CH_3^- ,²⁴ photoelectron spectroscopy on a system like this provides insights into the equilibrium geometry of the anion and the potential curve for the ν_2 mode in the neutral molecule. In this paper, the measured vertical detachment energy of SO_3 is compared with the results of DFT and ab initio calculations. Franck–Condon factors for the ν_1 and ν_2 modes have been calculated and used to analyze the experimentally observed vibrational structure.

2. Experimental Details

The photoelectron kinetic energy spectra of SO_3^- at 355 and 266 nm were measured with a fast-beam photoelectron spectrometer. The apparatus has been described in detail previously.^{25,26} Briefly, a mixture of Ar, N_2O and SO_2 expands into vacuum through a pulsed valve and subsequently passes through a pulsed electrical discharge²⁷ where negative ions are produced. The ions are cooled in a supersonic expansion, accelerated to 3 keV, mass-selected by time-of-flight and collimated before interaction with a polarized Nd:YAG laser beam (266 or 355 nm, 100 ps pulse width, ≈ 15 mJ/cm² fluence, 1 kHz repetition rate).

Photoelectrons are detected in the direction perpendicular to the plane of the laser and ion beams by a large, solid-angle, time- and position-sensitive detector.²⁵ Using the time-of-flight through a field-free region and the position of detection, the recoil angle of each photoelectron was calculated, allowing correction of the electron laboratory kinetic energy to the center-of-mass electron kinetic energy (eKE).²⁸ The present experi-

* Corresponding author. E-mail rcontinetti@ucsd.edu.

[†] Permanent address: Department of Chemistry, Chungnam National University, Taejon 305-764, Korea and Center for Molecular Science, 373–1 Kusung-dong, Yuseong-gu, Taejon 305-701, Korea.

ments were performed with the laser polarized either along the nominal axis of the photoelectron detector ($\theta = 0^\circ$) or perpendicular to the nominal detection axis, in the direction of the ion beam ($\theta = 90^\circ$). Calibration of the photoelectron spectra was performed by photodetachment of both O^- and S^- . The expected peaks in these atomic photoelectron spectra were reproduced with an accuracy of ~ 10 meV.

In the experiment, photoelectron spectra from two types of ions at $m/e = 80$ were detected: S_2O^- and SO_3^- . The photoelectron spectrum of the S_2O^- anion was recognized by observation of the ground electronic state of S_2O , as previously reported in a study of the photodetachment of S_2O^- in the visible region by Ellison and co-workers.²⁹ In the pulsed-discharge ion source, the relative intensities of these two components depended on the source gas mixture. The optimum gas mixture for the production of SO_3^- in the discharge was found to be 89% Ar, 9% N_2O , 2% SO_2 . Increasing the SO_2 concentration in the mixture led to an increase in the production of S_2O^- .

3. Computational Methods

To aid in interpretation of the measured photoelectron spectra, high-level quantum chemical calculations of the geometries, energetics, and vibrational frequencies of SO_3 and SO_3^- were made using the Gaussian 94 program suite³⁰ on a Cray C90 supercomputer installed at the Systems Engineering Research Institute (SERI), Korea. While extensive benchmark calculations by Martin on SO_3 have been performed,^{16,17} the primary goal of this study was to have a consistent ab initio treatment of both the anion and neutral geometries and energetics for comparison to experiment.

The geometric parameters for different choices of initial structural and electronic properties of SO_3 and SO_3^- were optimized using a gradient technique and the correlation consistent polarized valence double ζ (cc-pVDZ) and correlation consistent polarized valence triple ζ (cc-pVTZ) basis sets of Dunning³¹ at the MP2 (SO_3), UMP2 (SO_3^-),^{32–34} and DFT³⁵ levels. All inner-shell electrons were included in the correlation energy calculations for all of the configurations of SO_3 and SO_3^- .

For each structure, the harmonic vibrational frequencies were evaluated using the analytic second derivative technique at the (U)MP2/cc-pVDZ and B3LYP/cc-pVDZ levels. The harmonic vibrational frequencies were used to determine if a given structure was a local minimum on the potential energy surface and to perform zero point energy (ZPE) corrections.

To obtain more reliable energies, additional single point energy calculations were carried out for all of the species using the CCSD(T) (coupled-cluster with all single and double substitutions, and a quasi-perturbative estimate for the effect of connected triple excitations)^{36–40} method with the cc-pVTZ basis set. A number of studies show that the CCSD(T) method is a reliable and cost-efficient technique for ab initio quantum chemistry^{39,41} and that the CCSD(T) level of theory estimates energies very close to full configuration interaction³⁷ when nondynamical correlation effects are not very important.^{39,42} The inner-shell electrons are excluded from the correlation energy calculation at the CCSD(T) level on all species. Martin has shown that inner-shell correlation effects are important in SO_3 ,^{16,17} however, limited computation time prevented us from carrying out calculations including these interactions. The reliability of the single-reference correlation treatment was also checked by calculating the T_1 diagnostic.^{42,43} The T_1 diagnostic is a measure of the importance of nondynamic correlation and was found to be 0.0187 for SO_3 and 0.0197 for SO_3^- . Studies

TABLE 1: Geometrical Parameters of the Ground Electronic States of SO_3 and SO_3^-

species	symmetry	state	(U)MP2/ cc-pVDZ	B3LYP/ cc-pVDZ	(U)MP2/ cc-pVTZ	exp ^a
			$r_{SO}, \text{\AA}$	$r_{SO}, \text{\AA}$	$r_{SO}, \text{\AA}$	
Bond Lengths						
SO_3	D_{3h}	$^1A_1'$	1.469	1.468	1.439	1.41732
SO_3^-	C_{3v}	2A_1	1.520	1.533	1.485	
\angle OSO angle						
SO_3	D_{3h}	$^1A_1'$	120°	120°	120°	120°
SO_3^-	C_{3v}	2A_1	114.2°	113.6°	114.2°	

^a Reference 8.

have shown that if T_1 exceeds 0.02, the degree of multireference character is large enough to cast serious doubt on the reliability of single-reference correlation treatments.^{42,43} Since T_1 was found to be less than 0.02, the single-reference correlation treatment used in these MP2 and CCSD(T) calculations should be reasonable.

The calculated planar geometry of SO_3 is compared with experimental results reported in the literature in Table 1. Among the calculations, the (U)MP2/cc-pVTZ calculation yields a structure with an S–O bond length of 1.439 Å, which is in reasonable agreement with the experimental value of $r_e = 1.41732$ Å.⁹ This result is also consistent with the benchmark calculations of Martin, who found that use of progressively larger basis sets and inclusion of inner-shell correlation effects yielded progressively shorter bond lengths. His extensive CCSD(T)/MT-core calculations (using the Martin–Taylor basis set of spdgh quality, including inner-shell correlation effects) gave a theoretical S–O bond length of 1.41764 Å, for example. For SO_3 and SO_3^- the total energies from the calculations including ZPE are given in Table 2. In Table 3, the adiabatic electron affinity and vertical detachment energy (AEA and VDE, respectively) predicted at the various levels are given. To find the vertical detachment energy (VDE), the energy of the SO_3 neutral was calculated at the geometry of the SO_3^- anion. The AEA at the CCSD(T)/(U)MP2 level of 1.763 eV is significantly lower than that reported by McKee at a lower level of theory.²³ Table 4 summarizes the theoretical harmonic frequencies of both SO_3 and SO_3^- and compares those found in the present study of SO_3 with the spectroscopic-quality calculations of Martin.¹⁶ Further discussion of these calculations will be presented in the context of the experimental data in the following sections.

4. Experimental Results

The photoelectron spectra, $N(eKE)$, for $m/e = 80$ obtained in this experiment at 266 nm (4.66 eV) and separately measured spectra of S_2O^- and O^- are shown in Figure 1 for both laser polarizations. The photoelectron spectra of O^- were obtained from the same ion source, while the pure S_2O^- spectrum was obtained by production of $m/e = 80$ in a CS_2/N_2O gas mixture in a separate experiment.⁴⁴ Laser-correlated background at $eKE < 0.5$ eV has been subtracted from the data at 266 nm. In the $\theta = 90^\circ$ laser polarization spectrum shown in the upper frame, a broad peak at 1.0 eV is observed from a mixture of SO_3^- , S_2O^- , and O^- . A small, resolved contribution from excited states of S_2O can be seen near the origin of the eKE axis. The two sharp peaks at 1.23 and 3.20 eV are the well-known photodetachment peaks for $O^- + h\nu \rightarrow O(^3P, ^1D) + e^-$. The intensity of the O^- peaks was found to be proportional to the square of laser power, indicating that O^- is formed in the photodissociation of SO_3^- at 266 nm: $SO_3^- + h\nu \rightarrow SO_2 + O^-$, followed by photodetachment of the nascent O^- by a second photon. The $\theta = 0^\circ$ laser polarization spectrum in the lower

TABLE 2: Sum of Electronic and Zero Point Energies in Hartrees of the Ground States of SO_3 and SO_3^- ^a

species	sym.	state	(U)MP2/cc-pVDZ	B3LYP/cc-pVDZ	(U)MP2/cc-pVTZ	CCSD(T)/cc-pVTZ// (U)MP2/cc-pVTZ
SO_3	D_{3h}	$^1A_1'$	-622.702709	-623.765698	-623.098680	-623.050763
SO_3	C_{3v}	1A_1	-622.662851	-623.722496	-623.056891	-623.009865
SO_3^-	C_{3v}	2A_1	-622.739555	-623.833393	-623.155947	-623.115547

^a Zero point energy correction of the (U)MP2/cc-pVTZ and CCSD(T)/cc-pVTZ//MP2/cc-pVTZ energies were made using the (U)MP2/cc-pVDZ calculation at the (U)MP2/cc-pVTZ optimized geometry.

TABLE 3: Adiabatic Electron Affinity (AEA) and Vertical Detachment Energy (VDE) of SO_3A (in eV)

electron affinity	(U)MP2/ cc-pVDZ	B3LYP/ cc-pVDZ	(U)MP2/ cc-pVTZ	CCSD(T)/cc-pVTZ/ (U)MP2/cc-pVTZ	exp.
AEA	1.003	1.842	1.558	1.763	1.9 ^b
VDE	2.087	3.018	2.695	2.876	3.41 ^c
VDE-AEA	1.085	1.176	1.137	1.113	1.5 ^d

^a Zero point energy corrections to the (U)MP2/cc-pVTZ and CCSD(T)/cc-pVTZ//MP2/cc-pVTZ energies are from the (U)MP2/cc-pVDZ calculation. ^b Reference 21, ± 0.1 eV. ^c Present experiment, ± 0.01 eV. ^d Using the VDE from the present experiment and AEA = 1.9 eV from ref 21.

TABLE 4: Calculated Harmonic Frequencies for SO_3 and SO_3^- (unscaled)

	Neutral			
	SO_3	MP2/ cc-pVDZ ^a	B3LYP/ cc-pVDZ	Martin ^b CCSD(T)/ MTcore extrapolation
ν_1 (a_1') SO stretch		1108	998	1081.2
ν_2 (a_2') umbrella		434	453	503.1
ν_3 (e')		1492	1314	1415.1
ν_4 (e')		487	480	531.6
	Anion			
SO_3^-	UMP2/cc-pVDZ ^c	B3LYP/cc-pVDZ	UHF SCF ^d	
ν_1 (a_1) SO stretch	1062	899	1000	
ν_2 (a_1)	559	528	604	
ν_3 (e)	1284	1060	1175	
ν_4 (e)	452	433	511	

^a Frequency calculation at the MP2/cc-pVTZ-optimized geometry. ^b Reference 16. ^c Frequency calculation at the UMP2/cc-pVTZ-optimized geometry. ^d Reference 19.

frame of Figure 1 is dominated by the signal from SO_3^- , yielding a peak at 1.2 eV. This shows that the photoelectron angular distribution peaks along the electric vector of the laser, consistent with photodetachment from a totally symmetric A_1 orbital.⁴⁵ In the spectra shown in Figure 2, the contributions from S_2O^- and O^- have been subtracted, and the maximum of the SO_3^- photoelectron signal is found at 1.25 ± 0.01 eV, yielding an experimental vertical detachment energy (VDE) for SO_3 of 3.41 ± 0.01 eV.

The origin of the SO_3^- photoelectron spectrum cannot be observed directly in this experiment; however, the previously measured adiabatic electron affinity (AEA) of 1.9 ± 0.1 eV²¹ indicates that the origin of the 266 nm photoelectron spectrum is at 2.8 ± 0.1 eV. The large shift of the peak in the photoelectron spectrum to lower eKE from the EA indicates that the geometry of the anion is significantly different from the geometry of neutral molecule.

Vibrational structure is resolved in the 355 nm (3.49 eV) photoelectron spectrum shown in Figure 3. A comparison with the 266 nm spectra shows that the maximum intensity in the 355 nm spectrum is expected to be at eKE ≈ 0 eV, but the experimental spectrum is observed to drop in intensity approaching the origin. This is expected since electron transmission in the spectrometer decreases to zero at eKE = 0 eV. The

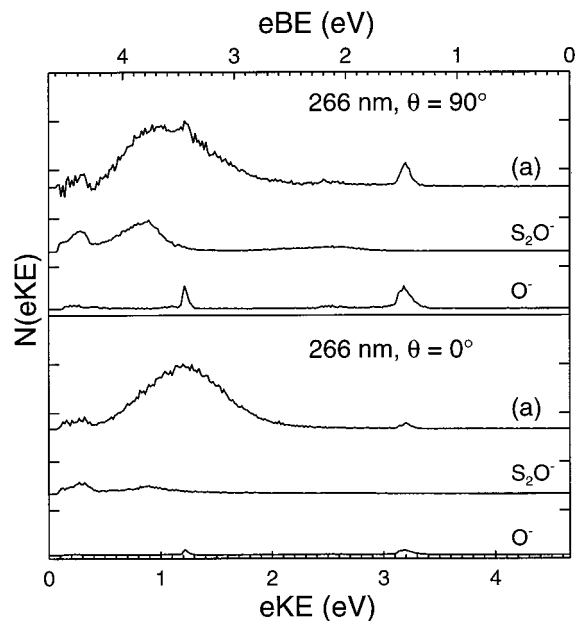


Figure 1. 266 nm photoelectron spectra, $N(eKE)$, observed for mixture of 89% Ar, 9% N_2O , and 2% SO_2 (curve (a) in each frame) and spectra of S_2O^- and O^- recorded in separate experiments (labeled and scaled to the top spectrum). Upper frame: laser polarization perpendicular to the nominal direction of electron detection ($\theta = 90^\circ$). Bottom frame: laser polarization parallel to the direction of electron detection ($\theta = 0^\circ$). Laser-related photoelectron background has been subtracted.

average peak spacing is 68 meV (550 cm^{-1}), close to the measured ν_2 (a_2' , 498 cm^{-1}) and degenerate ν_4 vibrations (e' , 530 cm^{-1}) known from infrared spectra (Table 4). Since the calculations described earlier predict a pyramidal structure (C_{3v} symmetry) for the SO_3^- anion and a planar structure for SO_3 (D_{3h}), significant excitation of ν_2 is expected after electron photodetachment.

The ν_2 vibrational frequency measured in the present experiment (550 cm^{-1}) is larger than the value of 498 cm^{-1} reported from high-resolution gas-phase infrared spectra.^{9,12} This discrepancy is close to the experimental uncertainty of 80 cm^{-1} in the present study, but possible origins for this difference should still be considered. The fundamental at 498 cm^{-1} is the accepted value for the harmonic frequency of ν_2 , although it was previously suggested to assign this frequency to the degenerate ν_4 vibration, and the 530 cm^{-1} vibrations to ν_2 .¹³ Since photodetachment of pyramidal SO_3^- produces planar SO_3 with many quanta in ν_2 excitation, the discrepancy between the present photoelectron data and the IR results may be a result of a positive quadratic or cubic anharmonicity constant. Such effects have been observed as a “negative anharmonicity” in the planar ground state of the methyl radical.⁴⁶ To explain the difference between the ν_2 fundamental previously measured and the result of the present experiment, a positive quadratic anharmonicity constant $x_{22} \approx 1.2 \text{ cm}^{-1}$ is required if $\nu_2(n+1 \leftarrow n) = \nu_2(1 \leftarrow 0) + 2n(x_{22})$, where n is the vibrational quantum number.⁴⁹ However, the experimental value for the quadratic anharmonicity constant obtained by Dorney et al.⁴⁹ from the

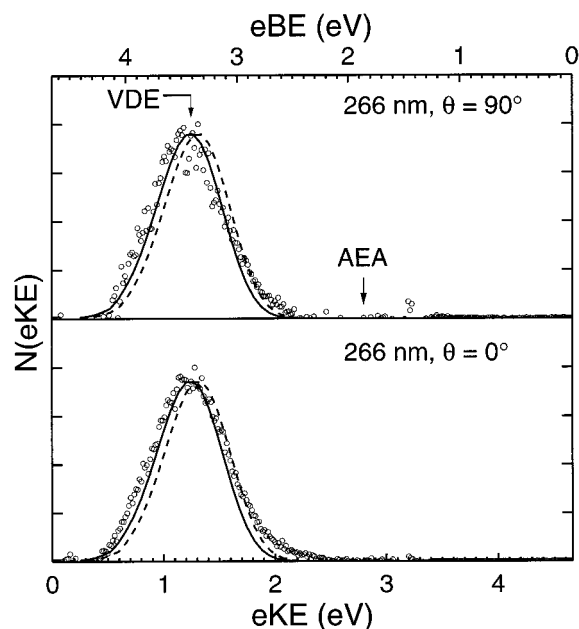


Figure 2. Photoelectron spectra of SO_3^- at 266 nm obtained from the difference between the total photoelectron spectrum (curves *a* in Figure 1) and the photoelectron spectra of S_2O_3^- and O^- . The Franck–Condon simulation is shown for both laser polarizations, along with the VDE and the AEA.²¹ The dashed line shows the Franck–Condon fit for AEA = 1.90 eV.²¹ The solid line shows the best Franck–Condon fit found using an assumed AEA = 1.97 eV.

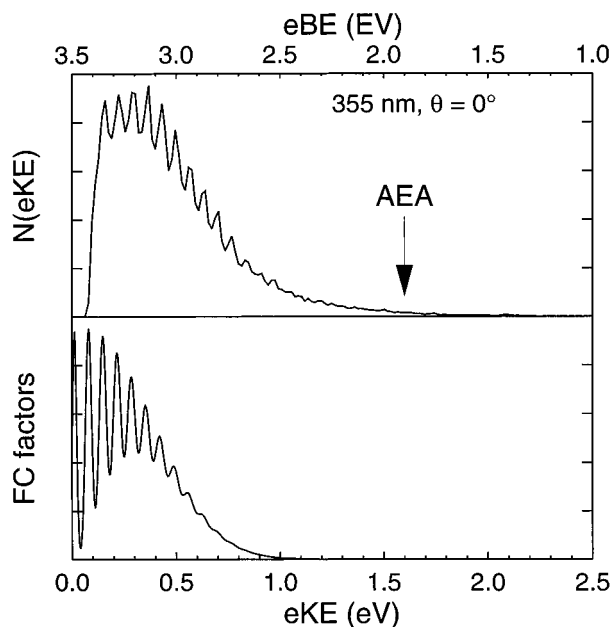


Figure 3. Upper frame: photoelectron spectrum of SO_3^- at 355 nm showing resolved ν_2 excitation. The laser polarization is in the direction of the photoelectron detector ($\theta = 0^\circ$). Bottom frame: photoelectron spectrum generated by the Franck–Condon simulation, dominated by the ν_2 mode, using the best-fit AEA = 1.97 eV.

gas-phase Raman spectrum gave a negative value of $x_{22} = -4.1 \text{ cm}^{-1}$. The recent spectroscopic-quality ab initio calculations by Martin¹⁶ of the quartic force field of SO_3 found the quadratic anharmonicity constant to be a factor of 4 smaller than Dorney et al.: $x_{22} = -0.75 \text{ cm}^{-1}$. Given this uncertainty in the quadratic anharmonicity, it is certainly possible that at the high levels of ν_2 excitation observed in the present experiment, reasonable quadratic or cubic anharmonicities may lead to the observed increase in spacing of the vibrational levels.

5. Comparison of Experimental and Ab Initio Results

Prior to considering any qualitative structural insights and explicit calculation of Franck–Condon factors for the photo-detachment of SO_3^- , it is useful to compare the calculated energetics presented earlier to the experimental results. The CCSD(T)/MP2/cc-pVTZ calculations are expected to yield the best energetics, and the AEA = 1.763 eV found by this method is closest to the published experimental values of $1.70 \pm 0.15 \text{ eV}$ ²⁰ and $1.9 \pm 0.1 \text{ eV}$.²¹ The calculated value for the VDE at this level of theory is 2.88 eV, (Table 3), significantly smaller than the value of $3.41 \pm 0.01 \text{ eV}$ observed in the present experiment. The DFT/cc-pVDZ calculations gave a somewhat larger value for the VDE of 3.018 eV, in better agreement with experiment, although this is likely to be fortuitous. This discrepancy between the experimental and theoretical values indicates the difficulty of carrying out accurate quantum chemistry calculations on molecules containing second-row elements such as SO_3^- and SO_3 , as discussed in some detail recently in Martin's benchmark study of SO_3 neutral.¹⁶

5.1. Analysis of the Vibrational Structure. Analysis of the vibrational structure observed in the photoelectron spectrum at 355 nm (Figure 3) provides additional information about the equilibrium geometry of SO_3^- . SO_3 can be examined as a classical harmonic oscillator prepared in a nonequilibrium configuration by Franck–Condon photodetachment of SO_3^- . Given the predicted geometry change between SO_3^- and SO_3 , significant excitation of the umbrella mode, ν_2 , is expected. Excitation of ν_2 can be analyzed classically following the approach taken by Yamada et al. in their study of CH_3 .⁴⁶ Displacement of the S atom along the z -axis perpendicular to the molecular plane can be approximated as the normal coordinate for ν_2 .⁴⁶ In the harmonic approximation, the vibrational frequency is $\nu_2 = (1/2\pi)(k_2/\mu)^{1/2}$, where $\mu = 3m_{\text{O}}m_{\text{S}}/(3m_{\text{O}} + m_{\text{S}})$ is the reduced mass, m_{O} and m_{S} are the masses of the oxygen and sulfur atoms respectively, and k_2 is the force constant. From the present experimental photoelectron spectrum, the vibrational quantum of ν_2 observed at high levels of excitation is $h\nu_2 = 0.068 \pm 0.010 \text{ eV}$ (or $\nu_2 = 548 \pm 80 \text{ cm}^{-1}$) and the corresponding force constant is $k_2 = 3.43 \pm 0.8 \text{ mdyne/\AA}$. Immediately after vertical photodetachment, the vibrational energy of SO_3 in the umbrella mode is then $E_{\text{vib}} = k_2 z^2/2$, where z is the equilibrium displacement of the S atom in SO_3^- from the plane of the oxygen atoms. A nominal experimental value for this vibrational energy can be found from the difference of the vertical and adiabatic electron affinities: $E_{\text{vib}} = \text{VDE} - \text{AEA}$, assuming that only ν_2 is excited upon photodetachment. From the literature AEA = $1.9 \pm 0.1 \text{ eV}$ ²¹ and the present experimental value for the VDE = $3.41 \pm 0.01 \text{ eV}$; this nominal peak vibrational energy is $E_{\text{vib}} = 1.5 \pm 0.1 \text{ eV}$. Given the experimentally observed vibrational quantum of 0.068 eV, this energy corresponds to the excitation of ≈ 22 ν_2 quanta in the harmonic approximation if it is assumed that only ν_2 is excited. This yields an S atom displacement of $z = 0.374 \pm 0.020 \text{ \AA}$, where the error is determined by the large experimental uncertainty in the force constant value k_2 . Within the limit of experimental error this value agrees well with the ab initio result, 0.366 \AA , obtained from the data given in Table 1 for the (U)-MP2/cc-pVTZ calculations.

5.2. Calculation of Franck–Condon Factors. The approach described by Chen⁴⁷ was employed to calculate explicit Franck–Condon factors for the excitation of SO_3 vibrations following photodetachment. This method allows excitation of several normal modes to be calculated and takes into account any mode-mixing effects arising from Duschinsky rotation⁴⁸ between the

anion and neutral normal modes. Using the experimentally known geometries and normal-mode frequencies for SO_3 and those calculated for SO_3^- (see Tables 1 and 4), the Franck–Condon factors for excitation of the ν_1 and ν_2 modes were calculated. Only the two normal modes of a_1' and a_2' symmetry were taken into account because excitation of the degenerate modes of e' symmetry (asymmetric stretch, ν_3 , and asymmetric bending, ν_4) is not allowed given the C_{3v} pyramidal symmetry of SO_3 immediately upon photodetachment. Excitation of these modes requires displacement of the S atom from the 3-fold molecular symmetry axis. Since both SO_3 and SO_3^- are expected to have 3-fold symmetry, and their ground electronic states are not degenerate, no Jahn–Teller distortions are expected. Thus, the 3-fold axial symmetry should be conserved upon photodetachment, and direct excitation of the ν_3 and ν_4 modes upon photodetachment is impossible.

To obtain the Franck–Condon factors, the geometry of SO_3^- , the vibrational frequencies and the Cartesian force constants were calculated at the (U)MP2/cc-pVDZ level as discussed earlier. In the Franck–Condon simulation, the anion was assumed to be in the lowest vibrational state. Although the CCSD(T)/(U)MP2/cc-pVTZ method gave better energetics, it would have been too expensive to obtain the Cartesian force constants at this level of theory.

The required structural parameters for SO_3 can also be taken from the ab initio calculations summarized in Tables 1 and 4; however, these calculated parameters deviate from the experimentally known values. For this reason, the experimentally derived normal modes and Cartesian force constants from the study of Dorney et al.⁴⁹ have been used in the present study, with the exception of the harmonic frequency of ν_2 , which has been taken as the present experimental value of 548 cm^{-1} . The values of Dorney et al. were calculated from the infrared and Raman spectra of SO_3 using an S–O bond length of $1.41 \pm 0.01\text{ \AA}$, which is close to $r_e = 1.41732\text{ \AA}$ reported later by Ortigoso et al.⁹ from high-resolution rotational spectra. To make use of the analysis by Dorney et al. it is important to consider the coordinate systems used for the neutral and anion and the transformations between normal, internal, and Cartesian coordinates. These considerations are described in the textbook of Wilson, et al.⁵⁰ and in a series of papers by McIntosh and Michaelian.⁵¹

The results of this simulation, using the theoretical predictions for SO_3^- and the experimental values for SO_3 , are shown in Figure 2 for both laser polarizations. The position of the 0–0 transition was determined from the experimentally known²¹ adiabatic electron affinity of $1.9 \pm 0.1\text{ eV}$. As expected, the calculation shows that predominantly ν_2 is excited after photodetachment. The Franck–Condon factors for excitation of $m\nu_1 + n\nu_2$ combination modes were found to be more than 10 times smaller than those for only ν_2 mode excitation, confirming the intuitive assumption that umbrella mode excitation occurs upon photodetachment of a pyramidal anion to a planar neutral molecule.

The simulated spectra reproduce the broad peak in the 266 nm spectrum quite well. The simulation using the literature value for the AEA = 1.9 eV is shown along with a best-fit simulation using the AEA = 1.97 eV with an estimated error of $\pm 0.1\text{ eV}$ given the uncertainties in the calculated geometries and force-constants of SO_3^- and SO_3 used in the Franck–Condon simulation. The vibrational structure resolved in the 355 nm spectrum is also reproduced reasonably well. Since the photoelectron transmission drops to zero for zero kinetic energy photoelectrons, the agreement in the overall shape of the

spectrum and the peak (predicted to be at $e\text{KE} = 0\text{ eV}$) is not as good as at 266 nm, as shown by the simulation in the lower frame of Figure 3. In addition, the Franck–Condon factor calculations did not include hot band transitions, which could account for some of the discrepancy between the simulated and experimental signal intensities at higher eKEs. To generate the simulations in Figures 2 and 3, the Franck–Condon factor for each vibrational peak is convoluted with a Gaussian function with an eKE-dependent width, as expected for a time-of-flight photoelectron spectrometer.⁵²

6. Discussion

In the present study we have shown how photodetachment from the SO_3^- anion produces SO_3 in highly vibrationally excited levels of ν_2 , not previously observed in IR and Raman spectroscopic studies of the ground state of SO_3 . To aid in the interpretation of the photoelectron spectra, ab initio and DFT calculations for both SO_3^- and SO_3 were carried out. For the SO_3 neutral, the calculations gave geometry and normal-mode frequencies reasonably close to the experimental values, but the reader is referred to the recent benchmark-quality calculations of Martin for the definitive study of SO_3 neutral.¹⁶ For the SO_3^- anion, these represent the highest-level calculations published to date. The calculations also reproduced the experimentally known AEA well. The largest discrepancy between the experimental results and the calculated energetics occurs in the VDE. This can result from either inaccuracies in the calculated equilibrium geometry of the anion or from problems in the calculation of the potential energy of the SO_3 neutral at the optimized geometry of anion.⁵³ It is more likely that the latter effect is responsible in this case, as at the geometry of the anion, SO_3 neutral is significantly displaced from its equilibrium position. As Table 3 shows, all applied methods underestimate the energy difference between planar and bent SO_3 by at least 0.39 eV. Since the S–O bond length was overestimated and the harmonic frequency of the SO_3 umbrella motion was underestimated in all calculations, it is possible that the difference between the potential energy of SO_3 in the equilibrium C_{3v} and photodetachment-excited D_{3h} configurations was underestimated as well, contributing to the error in the calculated vertical detachment energy. In any case, it is expected that SO_3 and SO_3^- represent challenging systems for accurate ab initio calculations. The discrepancies seen here between theory and experiment may be the result of basis-set limitations and the neglect of core-valence effects (inner-shell correlation) as discussed by Bauschlicher and co-workers in their study of SO and SO_2 .⁵⁴ Similarly, Martin has discussed the importance of polarization functions and augmented basis sets in his benchmark calculations on the neutral SO_3 molecule.^{8,16} More extensive calculations were beyond the scope of the present work; however, we hope that this work will motivate further theoretical studies of the SO_3^- anion.

As discussed in the experimental results section, photodissociation of SO_3^- to SO_2 and $\text{O}^-(^2\text{P})$ was observed at 266 nm. This excitation wavelength is close to the absorption peak of SO_3^- at 255 nm (molar absorptivity, $\epsilon = 1.15 \times 10^3\text{ M}^{-1}$) as observed by pulsed radiolysis in solution.¹⁰ Photodissociation of neutral SO_3 has been studied previously by photofragment translational spectroscopy.⁵⁵ After 193 nm excitation, the spin-allowed process $\text{SO}_3(X^1A_1') + h\nu \rightarrow \text{SO}_2(\tilde{X}^1A_1) + \text{O}(^1\text{D})$ was found to be the primary dissociation channel, requiring a photon energy of 5.56 eV. Two lower energy channels, the spin-forbidden photodissociation $\text{SO}_3(X^1A_1') + h\nu \rightarrow \text{SO}_2(\tilde{X}^1A_1) + \text{O}(^3\text{P})$ and the elimination of molecular oxygen, $\text{SO}_3(X^1A_1') +$

$h\nu \rightarrow \text{SO}(X^1\Sigma^-) + \text{O}_2(^3\Sigma_g^-)$, were not observed. In the photodissociation of SO_3^- , there are no spin restrictions for the lowest energy pathway, $\text{SO}_3^-(X^2A_1) + h\nu \rightarrow \text{SO}_2(\tilde{X}^1A_1) + \text{O}(^2P)$. The required energy can be calculated by considering the following thermodynamic cycle: the electron is removed from SO_3^- , SO_3 dissociates to $\text{SO}_2(\tilde{X}^1A_1) + \text{O}(^2P)$, ($D_0(\text{SO}_2-\text{O}) = 3.60$ eV), and finally the electron is added to the O atom. The first two steps require energy $\text{AEA}(\text{SO}_3) + D_0(\text{SO}_2-\text{O})$ and the last step releases energy of $\text{AEA}(\text{O})$. The AEA of the O atom is 1.46 eV.⁵⁶ Thus, the total energy required for the SO_3^- dissociation process is 3.84 eV, less than the 4.66 eV available with 266 nm excitation. The excess energy (0.82 eV) is insufficient to populate the low-lying electronic states of SO_2 which lie more than 3 eV above the ground state,⁵⁷ indicating that the observed photodissociation reaction is $\text{SO}_3^- + h\nu \rightarrow \text{SO}_2(\tilde{X}^1A_1) + \text{O}^-(^2P)$.

7. Conclusions

The photoelectron spectra of SO_3^- at 355 and 266 nm are reported in this paper. Vibrational structure, assigned to high levels of excitation in the ν_2 mode, was resolved in the 355 nm spectrum. Analysis of the photoelectron spectra supports theoretical predictions of the pyramidal structure of the SO_3^- anion. The photodissociation of $\text{SO}_3^- \rightarrow \text{SO}_2 + \text{O}^-(^2P)$ was also observed at 266 nm. The discrepancies between the theoretical predictions of the structure of SO_3^- and the experimental results discussed here highlight the difficulties associated with performing accurate ab initio calculations on molecules with third-row elements. Given the importance of SO_3 as an intermediate in the production of sulfuric acid in the atmosphere, future studies of $\text{SO}_3^- (\text{H}_2\text{O})$ complexes will be of interest.

Acknowledgment. This work was supported by the Chemistry Division of the National Science Foundation under grant CHE 97-00142. R.E.C. is a Camille Dreyfus Teacher-Scholar, an Alfred P. Sloan Research Fellow and a Packard Fellow in Science and Engineering. L.S.A. is supported by a Cota Robles Fellowship. B.H.B. is grateful to the Center for Molecular Science (CMS) for partial financial support. The computations were carried out on the CRAY C90 of the SERI Supercomputer center in Korea, which is gratefully acknowledged. We also thank Dr. Hans-Jürgen Deyerl and Prof. Peter Taylor for helpful discussions concerning ab initio methods.

References and Notes

- Wayne, R. P. *Chemistry of Atmospheres*, Oxford Science Publications/Clarendon Press: Oxford, 1991.
- Kolb, C. E.; Jayne, J. T.; Worsnop, D. R.; Molina, M. J.; Meads, R. F.; Viggiano, A. A. *J. Am. Chem. Soc.* **1994**, *116*, 10314.
- Jayne, J. T.; Pöschl, U.; Chen, Y.; Dai, D.; Molina, L. T.; Worsnop, D. R.; Kolb, C. E.; Molina, M. J. *J. Phys. Chem.* **1997**, *101*, 10000.
- Lovejoy, E. R.; Hanson, D. R.; Huey, L. G. *J. Phys. Chem.* **1996**, *100*, 19911.
- Pommerening, C. A.; Bachrach, S. M.; Sunderlin, L. S. *J. Phys. Chem. A* **1999**, *103*, 1214.
- Meijer, E. J.; Sprit, M. *J. Phys. Chem. A* **1998**, *102*, 2893.
- Morokuma, K.; Muguruma, C. *J. Am. Chem. Soc.* **1994**, *116*, 10316.
- Hofmann, M.; Schleyer, P. v. R. *J. Am. Chem. Soc.* **1994**, *116*, 4947.
- Ortigoza, J.; Escribano, R.; Maki, A. G. *J. Mol. Spec.* **1989**, *138*, 602.
- Lloyd, D. R.; Roberts, P. J.; Hillier, I. H.; Shenton, I. C. *Mol. Phys.* **1976**, *31*, 1549 and references therein.
- Henfrey, N. F.; Thrush, B. A. *Chem. Phys. Lett.* **1983**, *102*, 135.
- Kaldor, A.; Maki, A. G.; Dorney, A. J.; Mills, I. M. *J. Mol. Spec.* **1973**, *45*, 247.
- Thomas, R. K.; Thompson, H. *Proc. R. Soc. London A* **1970**, *314*, 329.
- Bondybey, V. E.; English, J. H. *J. Mol. Spec.* **1985**, *109*, 221.
- Jou, S.-H.; Shen, M.; Yu, C.; Lee, Y.-P. *J. Chem. Phys.* **1996**, *104*, 5745.
- Martin, J. M. L. *Spectrochim. Acta A* **1999**, *55*, 709.
- Martin, J. M. L. *Chem. Phys. Lett.* **1999**, *310*, 271.
- Hayon, E.; Treinin, A.; Wilf, J. *J. Am. Chem. Soc.* **1972**, *94*, 47.
- Stanbury, D. M.; Holme, T. A.; Kafafi, Z. H.; Margrave, J. L. *Chem. Phys. Lett.* **1986**, *129*, 181.
- Rothe, E. W.; Tang, S. Y.; Reck, G. P. *J. Chem. Phys.* **1975**, *62*, 3829.
- Miller, T. M.; Viggiano, A. A.; Arnold, S. T.; Jayne, J. T. *J. Chem. Phys.* **1995**, *102*, 6021.
- Ding, C.-F.; Wang, X.-B.; Wang, L.-S. *J. Chem. Phys.* **1999**, *110*, 3635.
- McKee, M. L. *J. Phys. Chem.* **1996**, *100*, 3473.
- Ellison, G. B.; Engelking, P. C.; Lineberger, W. C. *J. Am. Chem. Soc.* **1978**, *100*, 2556.
- Hanold, K. A.; Sherwood, C. R.; Garner, M. C.; Continetti, R. E. *Rev. Sci. Instrum.* **1995**, *66*, 5507.
- Zengin, V.; Persson, B. J.; Strong, K. M.; Continetti, R. E. *J. Chem. Phys.* **1996**, *105*, 9740.
- Osborn, D. L.; Leahy, D. J.; Cyr, D. R.; Neumark, D. M. *J. Chem. Phys.* **1996**, *104*, 5026.
- Hotop, H.; Lineberger, W. C. *J. Phys. Chem. Ref. Data* **1986**, *14*, 731.
- Nimlos, M. R.; Ellison, G. B. *J. Phys. Chem.* **1986**, *90*, 2574.
- Frisch, M. J.; Trucks, G. W.; Schlegel, H. B.; Gill, P. M. W.; Johnson, B. G.; Robb, M. A.; Cheeseman, J. R.; Keith, T.; Petersson, G. A.; Montgomery, J. A.; Raghavachari, K.; Al-Laham, M. A.; Zakrzewski, V. G.; Ortiz, J. V.; Foresman, J. B.; Cioslowski, J.; Stefanov, B. B.; Nanayakkara, A.; Challacombe, M.; Peng, C. Y.; Ayala, P. Y.; Chen, W.; Wong, M. W.; Andres, J. L.; Replogle, E. S.; Gomperts, R.; Martin, R. L.; Fox, D. J.; Binkley, J. S.; Defrees, D. J.; Baker, J.; Stewart, J. P.; Head-Gordon, M.; Gonzalez, C.; Pople, J. A. *Gaussian 94, Revision D.2*; Gaussian, Inc: Pittsburgh, PA, 1995.
- Woon, D. E.; Dunning, T. H., Jr. *J. Chem. Phys.* **1993**, *98*, 1358.
- Frisch, M. J.; Head-Gordon, M.; Pople, J. A. *Chem. Phys. Lett.* **1988**, *153*, 503.
- Frisch, M. J.; Head-Gordon, M.; Pople, J. A. *Chem. Phys. Lett.* **1990**, *166*, 281.
- Frisch, M. J.; Head-Gordon, M.; Pople, J. A. *Chem. Phys. Lett.* **1990**, *166*, 275.
- Parr, R. G.; Yang, W. *Density-functional theory of atoms and molecules*, Oxford University Press: Oxford, 1989.
- Raghavachari, K.; Trucks, G. W.; Pople, J. A.; Replogle, E. *Chem. Phys. Lett.* **1989**, *158*, 207.
- Watts, J. D.; Gauss, J.; Bartlett, R. J. *J. Chem. Phys.* **1993**, *98*, 8718.
- Seidl, E. T.; Schaefer, H. F. *J. Chem. Phys.* **1992**, *96*, 4449.
- Scuseria, G. E.; Lee, T. J. *J. Chem. Phys.* **1990**, *93*, 5851.
- Scuseria, G. E. *Chem. Phys. Lett.* **1991**, *176*, 27.
- Raghavachari, K.; Trucks, G. W.; Pople, J. A.; Head-Gordon, M. *Chem. Phys. Lett.* **1989**, *157*, 479.
- Lee, T. J.; Rendell, A. P.; Taylor, P. R. *J. Phys. Chem.* **1990**, *94*, 5463.
- Martin, J. M. L.; Slanina, Z.; Francois, J.-P.; Gijbels, R. *Mol. Phys.* **1994**, *82*, 155.
- Dobrin, S.; Continetti, R. E., unpublished work.
- Nimlos, N. R.; Ellison, B. *J. Am. Chem. Soc.* **1986**, *108*, 6522.
- Yamada, C.; Hirota, E.; Kawaguchi, K. *J. Chem. Phys.* **1981**, *75*, 5256.
- Kohn, D. W.; Robles, E. S. J.; Logan, C. F.; Chen, P. *J. Phys. Chem.* **1993**, *97*, 4936; Chen, P. In *Unimolecular and Bimolecular Reaction Dynamics*; Ng, C. Y., Baer, T., Powis, I., Wiley & Sons Ltd.: Chichester, 1994; pp. 371–425.
- Duschinsky, F. *Acta Phys. URSS* **1937**, *7*, 551.
- Dorney, A. J.; Hoy, A. R.; Mills, I. M. *J. Mol. Spec.* **1973**, *45*, 253.
- Wilson, E. B.; Decius, J. C.; Cross, P. *Molecular Vibrations*, Dover: New York, 1980.
- McIntosh, D. F.; Michaelian, K. H. *Can. J. Spec.* **1979**, *24*, 1. McIntosh, D. F.; Michaelian, K. H. *Can. J. Spec.* **1979**, *24*, 35; **1979**, *24*, 65.
- Metz, R. B.; Weaver, A.; Bradforth, S. E.; Kitsopoulos, T. N.; Neumark, D. M. *J. Phys. Chem.* **1990**, *94*, 1377.
- Yates, B. F.; Schaefer, H. F. *J. Chem. Phys.* **1994**, *100*, 4459.
- Bauschlicher, C. W.; Ricca, A. *J. Phys. Chem.* **1998**, *102*, 8044.
- Thelen, M. A.; Huber, J. R. *Chem. Phys. Lett.* **1995**, *236*, 558.
- Neumark, D. M.; Lykke, K. R.; Andersen, T.; Lineberger, W. C. *Phys. Rev. A* **1985**, *32*, 1890.
- Katagiri, H.; Sako, T.; Hishikawa, A.; Yazaki, T.; Onda, K.; Yamanouchi, K.; Yoshino, K. *J. Mol. Struct.* **1997**, *413*, 589.